Effects of Additional Linkers in Biphenyl-4,4′-dinitrene on the Low-Lying Singlet−Triplet Energy Gap and Zero-Field Splitting

Shigeaki Nimura,[†] Osamu Kikuchi,[†] Tsuguyori Ohana,[‡] Akira Yabe,[†,‡] Shigeo Kondo,[‡] and Masahiro Kaise*[,‡]

Department of Chemistry, University of Tsukuba, Tsukuba, Ibaraki 305, and National Institute of Materials and Chemical Research, Tsukuba, Ibaraki 305, Japan

Received: September 26, 1996; In Final Form: December 13, 1996[⊗]

Perturbation effects of additional linkers on the spin−spin coupling in biphenyl-4,4′-dinitrene (**1**) were examined by introducing a linking group between 2- and 2′-positions of **1**. Five different doubly linked systems showed triplet ESR spectra corresponding to quinonoid dinitrenes. Curie law analyses suggested that all those triplet states were thermally excited triplet states. In addition, the singlet−triplet energy gaps, which were determined by the Curie law analyses, were well correlated with their corresponding zero-field-splitting (zfs) *D* values. The result could be explained by the stability of dinitrene character which is estimated from the resonance energy of the intervening π-system. Our semiempirical molecular orbital calculations supported the experimental correlation between the singlet−triplet energy gap and the zfs *D* value.

Introduction

Along with the studies on the high-spin organic molecules, investigation of intramolecular spin−spin interactions is one of the most exciting research areas.[1−8] In the course of our research in aromatic dinitrenes, we have studied spin−spin interactions between two nitreno groups.[7,8] Dinitrenes with quinonoid structures such as biphenyl-4,4′-dinitrene (**1**) have two localized σ-spins which are coupled with the π-system by a one-center interaction. Their interesting features have been reported by several groups as follows.

Firstly, the experimental zero-field-splitting (zfs) *D* values were very large compared to the *D* values that are estimated theoretically by a point-dipole approximation.[2−7]

Secondly, we recently reported that the singlet−triplet energy gap and zfs *D* value have an interesting correlation in four types of quinonoid dinitrenes that have different distance between two localized σ-spins.[8] For the electronic structures of quinonoid dinitrenes, a contribution of dinitrene character, which has two unpaired electrons in the π-system in addition to two localized σ-spins, is expected in the total wave function. We showed that the difference of the contribution explains the correlation.

In this work, we introduced additional linkers to **1** (Scheme 1) to perturb the π-system, keeping the distance of two localized σ-spins. The effects of perturbation of these additional linkers on the contribution of the dinitrene character and the spin−spin interaction in **1** were examined by ESR measurements and molecular orbital calculations.

Results

Typical ESR spectra obtained by the photolyses of diazide precursors (**DA2**−**DA6**) are shown in Figures 1 and 2. The strong peaks in the $g = 2.00$ region are observed in all the cases. They are ascribed to impurities of radicals formed under the photochemical conditions used in this work.

In the region 500−700 mT, all the spectra showed two overlapped triplet XY transitions that are characteristic signals of mononitrenes. These zfs parameters are listed in Table 1.

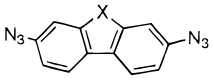

DA2; X=C_2H_2, **DA3**; X=S, **DA4**; X=O, **DA5**; X=CH_2, **DA6**; X=CO

The higher field signal grew, and subsequently the lower field ones grew. In addition, 2-azidofluorene (**A1**) and 2-azidofluorenone (**A2**) were irradiated by the same procedure. Each of the ESR spectra after the photolyses shows only one mononitrene resonance, which has the zfs *D* value 0.889 cm^{-1} (**A1**) or 0.881 cm^{-1}(**A2**), corresponding to the higher field signal of the dinitrene. These results show that the lower field resonances arise from secondary products such as 2-amino-7-nitrenofluorene, which is produced by the hydrogen abstraction of dinitrene from the matrix.

All the spectra, except the spectrum of **2**, show typical triplet resonances due to the quinonoid dinitrenes, but the peak positions are different from one another. Dinitrene **2** shows only a weak triplet XY transition at 467 mT. In the spectra of the quinonoid dinitrene in this work, the lower field XY transitions tend to be smaller and broader than the higher one, and thus the lower field XY transition of **2**, which is expected to appear at ca. 100 mT, is probably too weak to detect. In addition, no $|\Delta Ms| = 2$ line of **2** appeared because of the large zfs *D* value.

The zfs parameters of all the quinonoid dinitrenes were determined as listed in Table 2. The temperature dependence of these triplet signal intensities was measured three times independently for each dinitrene, as shown in Figure 3. To determine the singlet−triplet energy gaps of quinonoid dinitrenes, these plots were fitted by

$$I = (C/T)[3 \exp(-\Delta E/RT)/\{1 + 3 \exp(-\Delta E/RT)\}] \quad (1)$$

where *I* is the intensity, *C* is a constant, ΔE is the singlet−triplet energy gap, *R* is the gas constant, and *T* is the absolute temperature. The obtained energy gaps are listed in Table 2. The largest energy gap of **2** suggests the smallest population of triplet state, indicating the weak resonance intensity of the quinonoid triplet.

[†] University of Tsukuba.
[‡] National Institute of Materials and Chemical Research.
[⊗] Abstract published in *Advance ACS Abstracts,* February 15, 1997.

S1089-5639(96)02971-4 CCC: $14.00

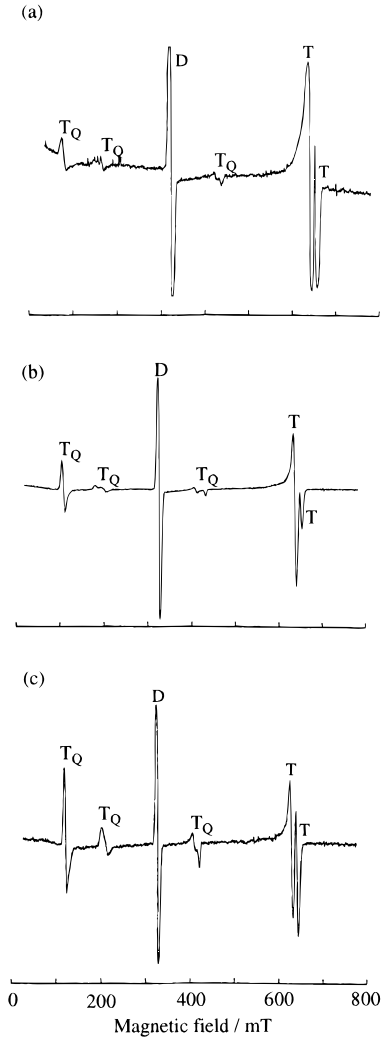

Figure 1. ESR spectra obtained after irradiation of (a) **DA3**, (b) **DA4**, and (c) **DA5**. Symbols T_Q, T, and D denote the triplet quinonid dinitrene, triplet mononitrene, and doublet radicals, respectively.

SCHEME 1

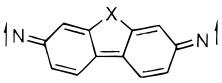

2; X=C_2H_2, **3**; X=S, **4**; X=O,
5; X=CH_2, **6**; X=CO

In the case of the photolyses of diazides **DA2** and **DA6**, the ESR spectra show additional strong signals in the lower regions (Figure 2). One of the possible origins of these peaks is products from side reactions. Those peaks could not be identified, although the following results led to the conclusion that these additional resonances were at least not ascribed to the quinonoid dinitrene: (1) the temperature dependence of the signal intensities followed the Curie law, indicating that these signals were resonances from ground state species, and (2) their irreversible decay rates were different from the quinonoid triplet signals.

Discussion

Figure 4 shows a correlation between the obtained singlet−triplet energy gaps and *D* values of the quinonoid dinitrene including **1**; that is, the energy gap increases as the *D* value gets larger. The correlation is comparable with that observed in stilbene-4,4′-dinitrene and azobenzene-4,4′-dinitrene.[8] Therefore the additional paths affect the total π-systems and then change the contribution of the dinitrene character in the total wave function.

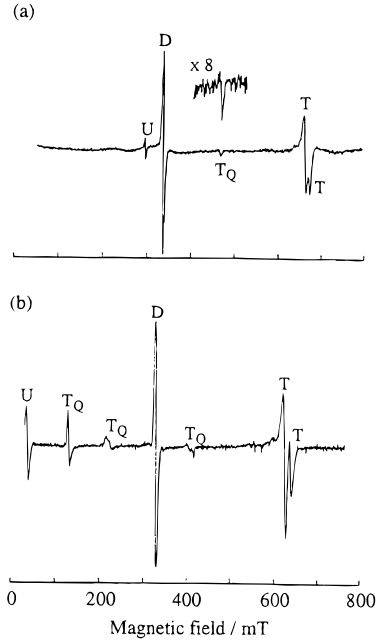

Figure 2. ESR spectra obtained after irradiation of (a) **DA2** and (b) **DA6**. Symbols T_Q, T, D, and U denote the triplet quinonid dinitrene, triplet mononitrene, doublet radicals, and unidentified signal, respectively.

TABLE 1: zfs Parameters of Mononitrenes

	zfs parameter[a]/cm^{-1}	
precursor photolyzed	lower field	higher field
DA2	0.897	0.936
DA3	0.891	0.927
DA4	0.868	0.914
DA5	0.834	0.878
DA6	0.814	0.864

[a] Zfs *E* parameters are almost zero. Lower field signals are due to byproducts.

TABLE 2: Singlet−Triplet Energy Gaps and zfs Parameters of Quinonoid Dinitrenes

compound	S−T gap[a]/kcal mol^{-1}	zfs parameter[b]/cm^{-1}
2	0.93 ± 0.05	0.286 (0.0)
3	0.88 ± 0.02	0.236 (0.037)
4	0.85 ± 0.01	0.205 (0.008)
5	0.78 ± 0.02	0.188 (0.004)
6	0.79 ± 0.01	0.174 (0.004)

[a] The values are average data from three plots. [b] Values in parentheses are zfs *E* values.

Then, why does the contribution of the dinitrene character change in each quinonoid dinitrene? The magnitude of resonance energies of intervening π-systems, such as fluorene in **5** connecting two nitreno groups, can be applied to this question. The first stabilizing factor of the dinitrene character is the preference of benzenoid structure. Thus the dinitrene character may depend on the resonance energy of the intervening π-system. Therefore, it is expected that as the resonance energies of these intervening π-systems increases, the contributions of dinitrene character increase. These resonance energies were calculated on the basis of the Hückel molecular orbital theory, as listed in Table 3. The order of these resonance energies is in accord with that of the *D* values and energy gaps.

Accordingly, the stability of benzenoid structure affects the contribution of the dinitrene character in the total wave function, and then the correlation between the *D* values and energy gaps appears.

Now let us look at the *D* values of mononitrene (Table 1). The order of these values is consistent with the order of the

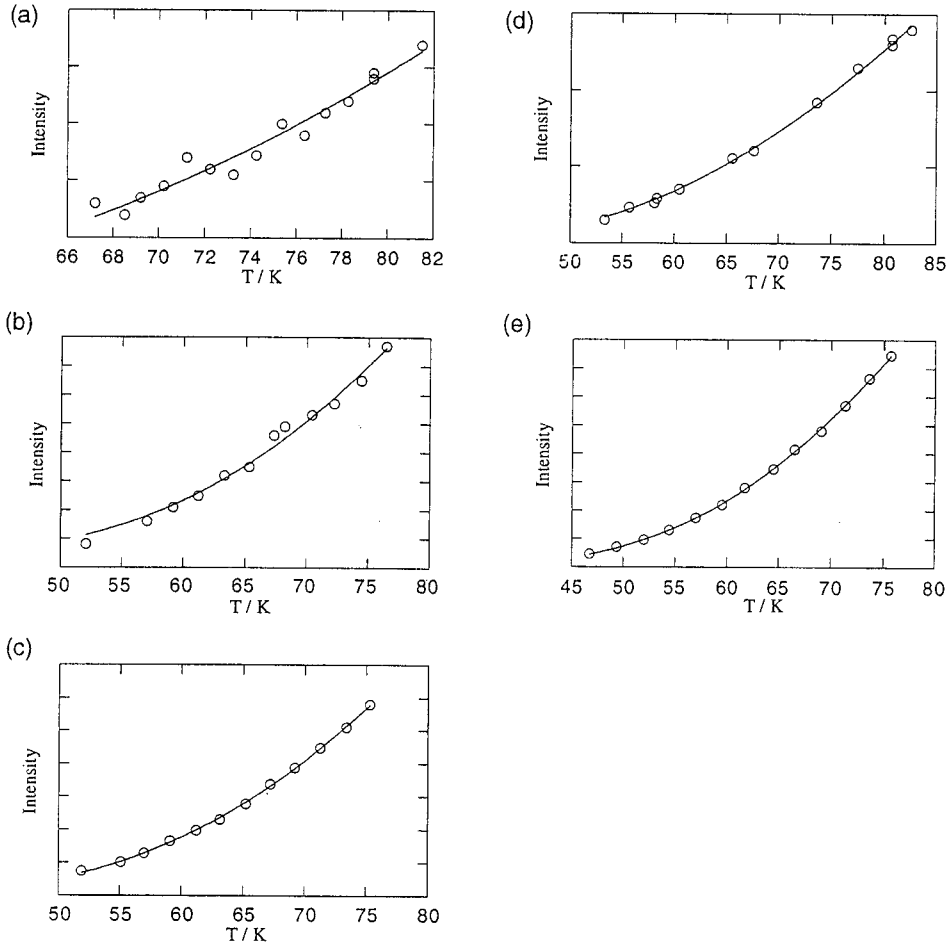

Figure 3. ESR signal intensities vs temperature of (a) **2**, (b) **3**, (c) **4**, (d) **5**, and (e) **6** with fitted curves. One of the three plots is shown for each compound.

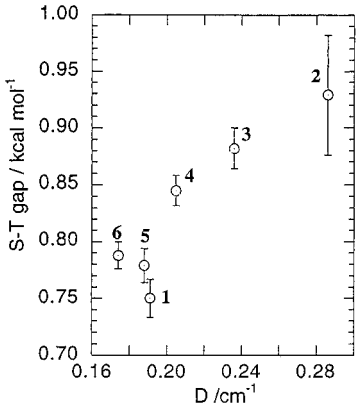

Figure 4. Relationship between the energy gap and zfs *D* value.

resonance energy of intervening π-systems. The large *D* values of these mononitrenes are mainly attributable to the resonance structure **7** (Scheme 3) because of a one-center interaction.[10] The contribution of structure **7**, which has a benzenoid structure, is dependent on the resonance energy. Therefore, in analogy with the quinonoid dinitnrene, the contribution of benzenoid structure affects the zfs *D* values.

Next, semiempirical molecular orbital calculations were carried out to clarify more detailed features of the electronic structures of the quinonoid dinitrenes. The principal configurations of the triplet state in the CI calculations are shown in Figure 5. The configurations **C** are related to the dinitrene character and thus prerequisite configurations to the large *D* values. Against the contributions of **C**, the calculated singlet−triplet energy gaps are plotted in Figure 6. Figure 6 shows a similar relationship as seen in Figure 4. These results support the above discussion of the relation between the *D* values and energy gaps.[11] In addition, C═N bond lengths are expected to be long as the contribution of the dinitrene character becomes large. The calculated lengths of the triplet states are almost the same, but the trend appears.

Finally, let us consider biphenylene-2,7-dinitrene (**10**), which has not yet been examined experimentally. Biphenylene, which is the intervening π-system of **10**, has the smallest resonance energy, as shown in Table 3, and thus a small contribution of the dinitrene character is expected in **10**. The PM3-CI calculation of **10** shows that the energy gap and the contribution of **C** are the smallest in these dinitrenes (Figure 6). This result is consistent with the smallest resonance energy of biphenylene.

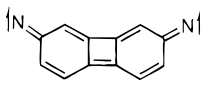

10

Conclusions

Despite the same distance of two localized σ-spins, the singlet−triplet energy gaps and zfs *D* values were changed and interrelated by the additional linkers in **1**. The correlation between the energy gaps and zfs *D* values was explained by the contribution of dinitrene character in the total wave function. Moreover, it is shown that the contribution of dinitrene character is attributable to the resonance energy of the intervening π-system. It is concluded that the crucial factor in the singlet−triplet energy gaps and *D* values in these systems is the stability of the dinitrene character.

SCHEME 2

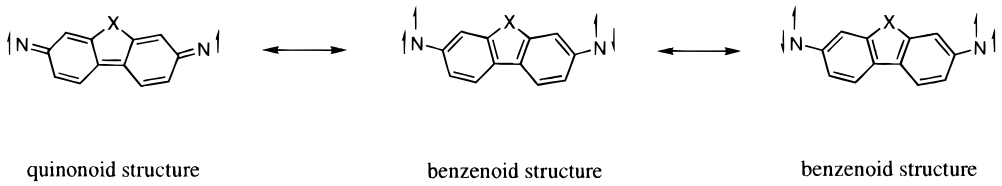

TABLE 3: Calculated Resonance Energies of Intervening π-System Skeletons

compound	resonance energy/β
phenanthrene	0.546[a]
dibenzothiophene	0.539
dibenzofuran	0.513
biphenyl	0.502[a]
fluorene	0.475
fluorenone	0.427
biphenylene	0.123[a]

[a] These data are taken from ref 9.

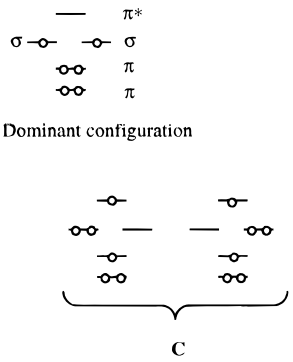

Figure 5. Schematic principal electron configurations of the triplet state in the CI calculations.

SCHEME 3

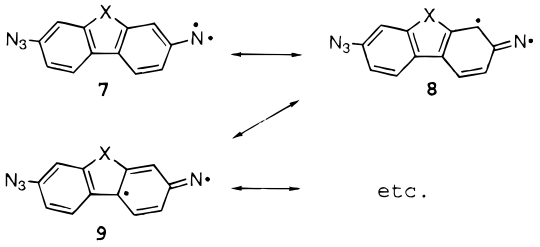

Experimental Section

General. ^{1}H and ^{13}C NMR spectra were recorded on a Bruker AC-200 spectrometer. IR spectra were obtained on a Shimadzu FTIR-8500. Mass spectra (MS) were recorded on a Shimadzu GCMS-QP1000EX gas chromatograph−mass spectrometer. Melting points were taken on a Yanagimoto Seisakusyo micro melting point apparatus and are uncorrected. High-resolution mass spectra (HRMS) were performed in the analytical center of the National Institute of Materials and Chemical Research. 2-Methyltetrahydrofuran was distilled from sodium.

2,7-Dinitro-9,10-dihydrophenanthrene. In a 100 mL Erlenmeyer flask was added 6 mL of fuming nitric acid with stirring over 3 h to a solution of 2.0 g (10 mmol) of 9,10-dihydrophenanthrene in 6 mL of glacial acetic acid, and the mixture was maintained at 45−50 °C. Some solid begins to separate after 1 h. The mixture was stirred for a further 3 h before cooling, and the resulting solid was washed thoroughly with water and dried. The obtained solid was crystallized from acetic acid to give 0.77 g (29%) of 2,7-dinitro-9,10-dihydrophenanthrene as pale yellow crystals: mp 222−223 °C (lit.[12] 226 °C); ^{1}H NMR ($CDCl_3$, 200 MHz) δ 3.07 (s, 4H), 7.94 (d, J = 8.5 Hz, 2H), 8.18−8.25 (m, 4H); ^{13}C NMR ($CDCl_3$, 50 MHz) δ 28.35, 122.58, 123.49, 125.57, 138.53, 139.39, 147.80.

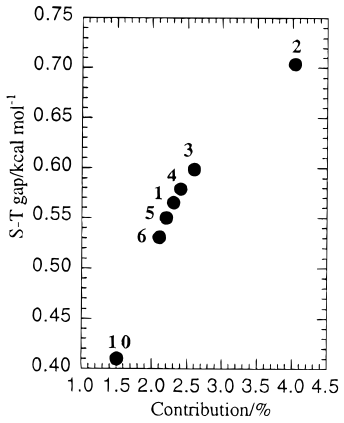

Figure 6. Relationship between the calculated singlet−triplet energy gap and the contribution of configuration **C**.

2,7-Dinitrophenanthrene. A mixture of 0.4 g (1.5 mmol) of 2,7-dinitro-9,10-dihydrophenanthrene, 0.26 g (1.5 mmol) of *N*-bromosuccinimide, a trace of dibenzoyl peroxide, and 10 mL of dry carbon tetrachloride was boiled under reflux for 3 h. The solid obtained on removal of the solvent from the filtered reaction mixture was crystallized from glacial acetic acid to give 0.2 g (50%) of 2,7-dinitrophenanthrene as bright yellow crystals: mp 337 °C (lit.[12] 333−336 °C); ^{1}H NMR ($CDCl_3$, 200 MHz) δ 8.04 (s, 2H), 8.53 (dd, J = 2.4 Hz, J = 8.9 Hz, 2H), 8.87 (d, J = 8.9 Hz, 2H), 8.88 (d, J = 2.4 Hz, 2H).

2,7-Diaminophenanthrene. A hot solution of 3.2 g (14 mmol) of stannous chloride dihydrate in 9 mL of concentrated hydrochloric acid was added during 1 min to a hot solution of 0.15 g (0.6 mmol) of 2,7-dinitrophenanthrene in 25 mL of acetic acid. After 3 min the solution was evaporated in vacuo. The residual oil was dissolved into water, and excess 50% aqueous sodium hydroxide was added. The liberated base was filtered, washed with alkali and then with water, and dried. The yield was 0.09 g (72%) of 2,7-diaminophenanthrene as a light yellow solid: ^{1}H NMR ($CDCl_3$, 200 MHz) δ 3.81 (br s, 4H), 7.00−7.04 (m, 4H), 7.47 (s, 2H), 8.31−8.36 (m, 2H).

2,7-Diazidophenanthrene (DA2). In a 100 mL Erlenmeyer flask were placed 25 mL of water, 7 mL of concentrated hydrochloric acid, and 0.07 g (0.34 mmol) of 2,7-diaminophenanthrene. The flask was placed in an ice-bath and treated dropwise with a solution of 0.1 g (1.4 mmol) of sodium nitrite in 10 mL of water. The mixture was stirred in the ice-bath for 1.5 h and then treated with a solution of 0.1 g (1.6 mmol) of sodium azide in 10 mL of water. The mixture was stirred for an additional 1 h and extracted with dichloromethane. The organic layer was dried over magnesium sulfate. The solvent was evaporated and recrystallized from ethanol to give 0.07 g (79%) of 2,7-diazidophenanthrene as light orange crystals: mp 131 °C (dec); IR (KBr, cm^{-1}) 2140; ^{1}H NMR ($CDCl_3$, 200 MHz) δ 7.32 (dd, J = 2.4 Hz, J = 8.8 Hz, 2H), 7.49 (d, J = 2.4 Hz, 2H), 7.69 (s, 2H), 8.57 (d, J = 8.8 Hz, 2H); ^{13}C NMR ($CDCl_3$, 50 MHz) δ 117.49, 119.21, 124.67, 127.61, 132.94, 138.55; HRMS calcd for $C_{14}H_8N_6$: 260.0810, found 260.0771.

3,7-Dinitrodibenzothiophene 5-oxide. A solution of 0.2 g (1 mmol) of dibenzothiophene-5-oxide in 7 mL of concentrated sulfuric acid was cooled to 12 °C and 4 mL of fuming nitric acid was added slowly so that the reaction temperature remained at 10−15 °C. The mixture was left at this temperature for 30 min. and then allowed to come to room temperature over 30 min. The precipitate obtained by pouring the nitration mixture on ice, was collected on a buchner, washed with water, and air dried to give 0.23 g (79 %) of 3,7-dinitrodibenzothiophene-5-oxide as pale yellow crystals: mp 258−259 °C (lit.[13] mp 257−258 °C); ^{1}H NMR ($CDCl_3$, 200 MHz) δ 8.13 (d, J = 8.6 Hz, 2H), 8.60 (dd, J = 2.1 Hz, J = 8.6 Hz, 2H), 8.94 (d, J = 2.1 Hz, 2H).

3,7-Diaminodibenzothiophene. A solution of 2 g (9 mmol) of stannous chloride dihydrate in 3 mL of concentrated hydrochloric acid was added to a hot solution of 0.23 g (0.8 mmol) of 3,7-dinitrodibenzothiophene 5-oxide in 4 mL of acetic acid and stirred 2 h at room temperature. Then the white suspension was heated at 100 °C and stirred for 1 h. After cooling to room temperature, the reaction mixture was filtrated and washed with brine. The solid was dispersed into water, and excess 40% aqueous sodium hydroxide was added. The mixture was filtered, washed with water, and dried to give 0.14 g (81%) of 3,7-diaminodibenzothiophene as a pale yellow solid: mp 169−170 °C (lit.[13] mp 169−170 °C); ^{1}H NMR ($CDCl_3$, 200 MHz) δ 3.77 (br s, 4H), 6.76 (dd, J = 2.1 Hz, J = 8.4 Hz, 2H), 7.05 (d, J = 2.1 Hz, 2H), 7.74 (d, J = 8.4 Hz, 2H).

3,7-Diazidodibenzothiophene (DA3). In a 200 mL Erlenmeyer flask were placed 50 mL of water, 15 mL of concentrated hydrochloric acid, and 0.14 g (0.65 mmol) of 3,7-diaminodibenzothiophene. The flask was placed in an ice-bath and treated dropwise with a solution of 0.15 g (2 mmol) of sodium nitrite in 25 mL of water. The mixture was stirred in the ice-bath for 1.5 h and then treated with a solution of 0.15 g (2 mmol) of sodium azide in 25 mL of water. The mixture was stirred for an additional 1 h and extracted with chloroform. The organic layer was dried over magnesium sulfate. The solvent was evaporated and recrystallized from ethanol to give 0.14 g (81%) of 3,7-diazidodibenzothiophene as a pale yellow solid: mp 161−162 °C; IR (KBr, cm^{-1}) 2130; ^{1}H NMR ($CDCl_3$, 200 MHz) δ 7.12 (dd, J = 2.1 Hz, J = 8.3 Hz, 2H), 7.46 (d, J = 2.1 Hz, 2H), 8.01 (d, J = 8.3 Hz, 2H); ^{13}C NMR ($CDCl_3$, 50 MHz) δ 112.69, 116.42, 122.27, 132.16, 138.70, 140.72; HRMS calcd for $C_{12}H_8N_6S$ 266.0374, found 266.0353.

3,7-Diaminodibenzofuran. A mixture of 8 g (21 mmol) of 4,4′-diamino-2,2′-biphenyldisulfonic acid and 70 g of 50% aqueous sodium hydroxide was heated at 280 °C (24−30 kg/cm^2) for 16 h in a 100 mL autoclave. After the mixture had been cooled, 400 mL of water was added. The mixture was filtrated, washed with water, and dried to give 0.85 g (20%) of 3,7-diaminodibenzofuran as a brown solid: mp 152−155 °C (lit.[14] 152 °C); ^{1}H NMR ($CDCl_3$, 200 MHz) δ 3.81 (br s, 4H), 6.67 (dd, J = 8.0 Hz, J = 4.0 Hz, 2H), 6.82 (d, J = 4.0 Hz, 2H), 7.54 (d, J = 8.0 Hz, 2H); ^{13}C NMR ($CDCl_3$, 50 MHz) δ 98.10, 111.24, 116.70, 120.16, 145.35, 157.80.

3,7-Diazidodibenzofuran (DA4). In a 200 mL Erlenmeyer flask were placed 100 mL of water, 10 mL of concentrated hydrochloric acid, and 0.4 g (2 mmol) of 3,7-diaminodibenzofuran. The flask was placed in an ice-bath and treated dropwise with a solution of 0.5 g (7 mmol) of sodium nitrite in 10 mL of water. The mixture was stirred in the ice-bath for 1.5 h and then treated with a solution of 0.6 g (9 mmol) of sodium azide in 10 mL of water. The mixture was stirred for an additional 30 min and extracted with ether. The organic layer was dried over magnesium sulfate. The solvent was evaporated and recrystallized from hexane to give 0.22 g (44%) of 3,7-diazidodibenzofuran as a yellow solid: mp 127−128 °C; IR (KBr, cm^{-1}) 2140; ^{1}H NMR ($CDCl_3$, 200 MHz) δ 7.03 (dd, J = 2.0 Hz, J = 8.0 Hz, 2H), 7.22 (d, J = 2.0 Hz, 2H), 7.84 (d, J = 8.0 Hz, 2H); ^{13}C NMR ($CDCl_3$, 50 MHz) δ 102.56, 114.57, 121.04, 121.16, 139.28, 157.32; HRMS calcd for $C_{12}H_6N_6O$ 250.0603, found 250.0590.

2,7-Diazidofluorene (DA5). In a 50 mL Erlenmeyer flask were placed 4 mL of water, 2 mL of concentrated hydrochloric acid, and 0.2 g (1 mmol) of 2,7-diaminofluorene. The flask was placed in an ice-bath and treated dropwise with a solution of 0.2 g (3 mmol) of sodium nitrite in 2 mL of water. The mixture was stirred in the ice-bath for 1 h and then treated with a solution of 0.2 g (3 mmol) of sodium azide in 2 mL of water. The mixture was stirred for an additional 15 min and extracted with ether. The organic layer was dried over magnesium sulfate. The solvent was evaporated and recrystallized from a mixture of ether and hexane to give 0.1 g (40%) of 2,7-diazidofluorene as orange crystals: mp 127; IR (KBr, cm^{-1}) 2120; ^{1}H NMR ($CDCl_3$, 200 MHz) δ 3.85 (s, 2H), 7.03 (d, J = 8.0 Hz, 2H), 7.16 (s, 2H), 7.66 (d, J = 8.0 Hz, 2H); ^{13}C NMR ($CDCl_3$, 50 MHz) δ 36.76, 115.74, 118.0, 120.64, 138.16, 138.43, 144.79; HRMS calcd for $C_{13}H_8N_6$ 248.0810, found 248.0815.

2,7-Diazidofluorenone (DA6). A hot solution of 5.0 g (22 mmol) of stannous chloride dihydrate in 6 mL of concentrated hydrochloric acid was added during 1 min to a hot solution of 1.0 g (3 mmol) of 2,7-dinitrofluorenone in 10 mL of acetic acid. After 5 min the solution was evaporated in vacuo. The residual oil was dissolved into water, and excess 50% alkali was added. The liberated base was filtered, washed with alkali and then with water, and dried, yielding 0.62 g (80%) of 2,7-diaminofluorenone as a brown solid: MS, *m/z* 210 (M^+).

In a 500 mL Erlenmeyer flask were placed 100 mL of water, 4 mL of concentrated hydrochloric acid, and 0.62 g (3 mmol) of 2,7-diaminofluorenone. The flask was placed in an ice-bath and treated dropwise with a solution of 0.5 g (7 mmol) of sodium nitrite in 10 mL of water. The mixture was stirred in the ice-bath for 2 h and then treated with a solution of 0.5 g (8 mmol) of sodium azide in 10 mL of water. The mixture was stirred for an additional 1 h and extracted with chloroform. The organic layer was dried over magnesium sulfate. The solvent was evaporated to give 0.52 g (66%) of 2,7-diazidofluorenone as an orange solid: mp 187 °C (dec); IR (KBr, cm^{-1}) 2130; ^{1}H NMR ($CDCl_3$, 200 MHz) δ 7.10 (dd, J = 8.0 Hz, J = 2.0 Hz, 2H), 7.33 (d, J = 2.0 Hz, 2H), 7.44 (d, J = 8.0 Hz, 2H); ^{13}C NMR ($CDCl_3$, 50 MHz) δ 115.228, 121.36, 124.91, 135.82, 140.49, 141.11, 191.889; HRMS calcd for $C_{13}H_6N_6O$ 262.0603, found 262.0613.

2-Azidofluorene (A1). In a 100 mL Erlenmeyer flask were placed 20 mL of water, 10 mL of concentrated hydrochloric acid, and 0.4 g (2.2 mmol) of 2-aminofluorene. The flask was placed in an ice-bath and treated dropwise with a solution of 0.2 g (3 mmol) of sodium nitrite in 5 mL of water. The mixture was stirred in the ice-bath for 1.5 h and then treated with a solution of 0.2 g (3 mmol) of sodium azide in 5 mL of water. The mixture was stirred for an additional 2 h and extracted with ether. The organic layer was dried over magnesium sulfate. The solvent was evaporated and recrystallized from hexane to give 0.4 g (86%) of 2-azidofluorene as a pale yellow solid: mp 105 °C (dec); IR (KBr, cm^{-1}) 2110; ^{1}H NMR ($CDCl_3$, 200 MHz) δ 3.83 (s, 2H), 7.00 (dd, J = 2.0 Hz, J = 8.1 Hz, 1H), 7.16 (s, 1H), 7.22−7.39 (m, 2 H), 7.50 (d, J = 7.3 Hz, 1H), 7.66−7.71 (m, 2H); ^{13}C NMR ($CDCl_3$, 50 MHz) δ 36.83, 115.71, 117.81, 119.63, 120.83, 125.01, 126.64, 126.91, 138.43, 138.92, 140.92, 142.89, 145.09; HRMS calcd for $C_{13}H_9N_3$ 207.0798, found 207.0765.

2-Azidofluorenone (A2). In a 100 mL Erlenmeyer flask were placed 10 mL of water, 1 mL of concentrated hydrochloric acid, and 0.3 g (1.5 mmol) of 2-aminofluorenone. The flask was placed in an ice-bath and treated dropwise with a solution of 0.15 g (2 mmol) of sodium nitrite in 5 mL of water. The mixture was stirred in the ice-bath for 1.5 h and then treated with a solution of 0.13 g (2 mmol) of sodium azide in 5 mL of water. The mixture was stirred for an additional 1 h and extracted with ether. The organic layer was dried over magnesium sulfate. The solvent was evaporated and recrystallized from hexane to give 0.33 g (99%) of 2-azidofluorenone as a yellow solid: mp 117−119 °C; IR (KBr, cm^{-1}) 2100; ^1H NMR ($CDCl_3$, 200 MHz) δ 7.06 (d, J = 7.2 Hz, 1H), 7.30 (s, 2H), 7.43−7.52 (m, 3H), 7.63 (d, J = 7.2, 1H); ^{13}C NMR ($CDCl_3$, 50 MHz) δ 114.87, 120.11, 121.46, 124.52, 128.84, 134.00, 135.01, 135.84, 140.76, 141.17, 144.03, 192.79; HRMS calcd for $C_{13}H_7N_3O$ 221.0589, found 221.0587.

ESR Measurement. ESR spectra were measured on a JEOL JES-RE3X spectrometer equipped with an optical transmission cavity and an Air Products LTD-3 liquid helium transfer system. The microwave frequency was measured with a Hewlett Packard 5340A frequency counter, and the resonance magnetic field values of the signals were measured with the aid of an Echo Electronics Co., Ltd., EFM-2000 NMR field meter.

Sample temperature was controlled with gas flow rates and a temperature controller. The temperature was monitored continuously just below the sample position in the cryostat. In addition, the temperature at the actual position was calibrated by measuring temperature with a chromel-AuFe thermocouple placed in the sample tube before each ESR experiment. The temperature was controlled with an Oxford ITC 503 temperature controller and an Advantest TR2114H temperature measurement with a chromel-AuFe thermocouple.

Appropriate diazide precursors were dissolved in purified 2-methyltetrahydrofuran. The solution (ca. 10^{-3} mol dm^{-3}) was placed in a quartz 4 mm o.d. ESR sample tube and degassed by freeze−pump−thaw cycles. The diazide precursors were irradiated with an USHIO UI-501C xenon lamp through Toshiba UV-D33S and UV-27 cutoff filters (270 nm < λ < 400 nm) to generate the dinitrenes. Photolysis of the various diazide precursors was carried out at various temperatures between 60 and 77 K and maintained at each temperature for at least 30 min before analyzing the ESR spectral behavior. The measurements were carried out at an appropriate low microwave power under each measurement condition to avoid the signal saturation effect.

Molecular Orbital Calculation. The molecular orbital calculations were carried out by a semiempirical method with the MOPAC ver. 6.0 program package.[15] All calculations were performed on IBM RS/6000 workstations or the Cray C90 supercomputer at RIPS of the Agency of Industrial Science and Technology. In the semiempirical computations the geometry of the triplet state of each molecule was optimized using a restricted open-shell wave function employing the PM3 Hamiltonian. Then configuration interaction calculations were carried out to compute the energy differences between the triplet and singlet states at the optimized geometries. Each state was assumed to be open-shell, with a five-orbital and six-electron active space.

The resonance energies were also calculated by a program written by Oka et al.[16] on an NEC 9801 microcomputer. Hückel parameters of the heteroatoms and the hyperconjugation of the CH_2 group are taken from ref 17.

Acknowledgment. We thank Dr. Takaaki Hanaoka, National Institute of Materials and Chemical Research, for assistance in the syntheses.

References and Notes

(1) Iwamura, H.; Miller, J. S., Eds. Proceedings of the Symposium on Ferromagnetic and High Spin Molecular Based Materials, *Mol. Cryst. Liq. Cryst*. **1993**, *232*, *233*.

(2) Trozzolo, A. M.; Murray, R. W.; Smolinsky, G.; Yager, W. A.; Wasserman, E. *J. Am. Chem. Soc.* **1963**, *85*, 2526.

(3) Singh, B.; Brinen, J. S. *J. Am. Chem. Soc.* **1971**, *93*, 540.

(4) Minato, M.; Lahti, P. M.; van Willigen, H. *J. Am. Chem. Soc.* **1993**, *115*, 4532.

(5) Ichimura,A. S.; Lahti, P. M. *Mol. Cryst. Liq. Cryst.* **1993**, *233*, 33.

(6) Minato, M.; Lahti, P. M. *J. Phys. Org. Chem.* **1993**, *6*, 483.

(7) Ohana, T.; Nimura, S.; Kikuchi, O.; Kaise, M.; Yabe, A. *Chem. Lett.* **1993**, 765.

(8) Nimura, S.; Kikuchi, O.; Ohana, T.; Yabe, A.; Kaise, M. *Chem. Lett.* **1996**, 125.

(9) Aihara, J. *J. Am. Chem. Soc.* **1976**, *98*, 2750.

(10) Coope, J. A. R.; Farmer, J. B.; Gardner, C. L.; McDowell, C. A. *J. Chem. Phys.* **1965**, *42*, 54.

(11) For electronic structures of diradical and dicarbene intermediates, more detail and extensive semiempirical molecular orbital calculations have been performed by C. Kollmar. His work was much benefit to us in the calculations: Kollmar, C. *J. Chem. Phys.* **1993**, *98* (9), 7210.

(12) Hallas, G.; Wada, B. T. *Chem. Ind.* **1978**, 630.

(13) Brown, R. K.; Nelson, N. A.; Wood, J. C. *J. Am. Chem. Soc.* **1952**, *74*, 1165.

(14) Wirth, H. O.; Waese, G.; Kern, W. *Makromol. Chem.* **1965**, *86*, 139.

(15) Stewart, J. J. P. *J. Comput. Chem.* **1989**, 10, 209, 221.

(16) Oka, O.; Takashima, H.; Aihara, J. *Kagaku* **1985**, *40* (1), Appendix 1 (in Japanese).

(17) (a) Hess, B. A., Jr.; Schaad, L. J.; Holyoke, C. W., Jr. *Tetrahedron* **1972**, *28*, 3657, 5299. (b) Hess, B. A., Jr.; Schaad, L. J. *J. Am. Chem. Soc.* **1973**, *95*, 3907. (c) Brauer, H.-D.; Reinsch, E.-A. *Ber. Bunsen-Ges.* **1973**, *77* (5), 348.